NPS ARCHIVE
1968
BECK, G.

AN EXPERIMENTAL DETERMINATION OF TWO DIMENSIONAL RIBBED WALL DIFFUSOR PERFORMANCE

GARY LAURENCE BECK

AN EXPERIMENTAL DETERMINATION OF TWO DIMENSIONAL RIBBED WALL DIFFUSOR PERFORMANCE

by

Gary Laurence Beck
Lieutenant, United States Navy
B.S., Central Michigan University, 1958

Submitted in partial fulfillment of the
requirements for the degree of

MASTER OF SCIENCE IN AERONAUTICAL ENGINEERING

from the

NAVAL POSTGRADUATE SCHOOL
March 1968

NPS ARCHIVE
968
BECK, G.

B 3275
C.1

ABSTRACT

The results of tests made with a two dimensional diffusor operating with transverse grooves cut into the diverging side walls were compared with the results of similar tests made using a smooth wall diffusor. The results of this comparison revealed that:

1. The efficiency of the ribbed wall configuration exceeded that of the smooth wall diffusor for total opening angles of approximately 28 to 33 degrees.

2. The ribbed wall configuration had an efficiency approximately 120 per cent of that of the smooth wall diffusor when both were operated at a total opening angle of 32 degrees.

3. The efficiencies of the ribbed wall diffusor operating at large opening angles varied as a function of the number of grooves in the side walls.

4. The efficiency increased as the number of grooves increased, but an unexplained drop in efficiency occurred at opening angles of 30 and 32 degrees with an eight groove configuration.

5. The maximum number of grooves tested was ten. There is no evidence to indicate that this is an optimum configuration.

TABLE OF CONTENTS

CHAPTER		PAGE
I.	INTRODUCTION	11
II.	EXPERIMENTAL PROCEDURES	17
	2.1 Experimental set-up	17
	2.2 Pressure readings	17
	2.3 Temperature measurements in the flow field	19
	2.4 Measuring and recording the data	19
III.	COMPUTATIONS AND ANALYSIS	23
	3.1 Temperature measurement conversions	23
	3.2 Pressure measurement conversions	23
	3.3 Flow rate measurements	23
	3.4 Flow conditions at the diffusor inlet	26
	3.5 Integrated flow rate at the diffusor inlet	27
	3.6 Diffusor performance	36
	3.7 Measurement reliability indicator	38
IV.	RESULTS AND RECOMMENDATIONS	39
	4.1 Results	39
	4.1.1 Preliminary phase	39
	4.1.2 Determination of the most desirable operating range	40
	4.1.3 Effect of varying the number of grooves upon ribbed wall diffusor performance	45
	4.2 Recommendations	45
	REFERENCES	48
	APPENDIX	49
	A. Computer program	49
	B. Computer program listing	56

LIST OF TABLES

TABLE		PAGE
I.	Summary of Two Dimensional Diffusor Studies from Reference 1	16
II.	Summary of Flow Rate Calculation Coefficients. .	25
III.	Summary of Continuity Calculations	36
IV.	Results of Repetitive Tests under Similar Operating Conditions	41
V.	Comparison of Smooth Wall and Ribbed Wall Diffusor Efficiencies.	42
VI.	Effect of Varying the Number of Grooves upon the Performance of a Ribbed Wall Diffusor. . . .	46

LIST OF FIGURES

FIGURE		PAGE
1.	Two Dimensional Diffusor and Detail of a Ribbed Wall Configuration	13
2.	Illustration of an Asymmetric Two Dimensional Diffusor of the Type Used in Ref. 1 and a Symmetric Two Dimensional Diffusor of the Type Used in This Study	15
3.	Schematic of the Experimental Installation Housed in the "New Addition" Building 230, Jet Propulsion Laboratory, NPGS, Monterey	18
4.	Schematic of the Diffusor Inlet Plane Illustrating the Location of the Total and Static Pressure Taps	20
5.	Schematic of the Pressure Instrumentation Installation	21
6.	Diffusor Inlet Velocity Profile at Mid-Span of Top Wall with Exponential Expression Used to Approximate the Shape of Profile	29
7.	Diffusor Inlet Velocity Profile at Mid-Span of Side Wall with Exponential Expression Used to Approximate the Shape of Profile	30
8.	Inlet Plane of Diffusor Showing the Location of Boundary Layers and Flow Regions as Used in the Determination of the Flow Rate Through the Inlet	32
9.	Corner Region (E) of the Inlet Plane	34
10.	Measured and the Predicted Velocities along the Corner Survey Path Line	35
11.	Summary of Ribbed Wall and Smooth Wall Diffusor Efficiencies	43
12.	Ratio η_R/η_S as a Function of β to Compare the Ribbed Wall Diffusor to That of a Smooth Wall Diffusor	44
13.	Sample Data Sheet	51
14.	Input Data Field and Format Specifications for Program DIFFUSOR	52
15.	Sample Output from Program DIFFUSOR	54

LIST OF SYMBOLS

SYMBOL	VALUES OR UNITS	DESCRIPTION
a	ft/sec	speed of sound
A	inches	depth of diffusor grooves
B	inches	width of diffusor grooves
C_{pr}	$\frac{P_2 - P_1}{q_1}$	coefficient of pressure recovery
D	$\frac{4 \times \text{Area}}{\text{Circumference}}$	equivalent diameter
g_c	$32.17 \frac{lbm\ ft}{lb_f\ Sec^2}$	conversion factor (Engineering to English units)
h	inches	boundary layer measurement, distance from wall
J	$778.3 \frac{ft\text{-}lb_f}{BTU}$	energy conversion factor
L	inches	length
M	$\frac{V}{a}$	Mach number
N		number of diffusor grooves
P_t	psia	total pressure
P	psia	static pressure
ΔP	psi	pressure difference or drop between two points in the flow
q	psi	dynamic head ($q = P_t - P$)
R_g	$53.35 \frac{ft\ lb_f}{lb_m\ °R}$	gas constant for air
Re	$\frac{VD}{\nu}$	Reynolds number based upon the equivalent diameter
T	°Rankine	temperature
t	°Fahrenheit	temperature

SYMBOL	VALUES OR UNITS	DESCRIPTION
TH	inches	thickness of wall between diffusor grooves
V	ft/sec	velocity
$\dot{w}$	lb_m/sec	mass flow rate
$\overset{*}{w}$	$in.^2$	equivalent flow rate
γ	1.4	ratio c_p/c_v
α	$\beta/2$	diffusor half-angle
β	degrees	total diffusor opening angle
ν	(funct. of temp.)	kinematic viscosity
ρ	slugs = $\frac{lb_f\ sec^2}{ft^4}$	density of fluid
η	$\frac{P_2 - P_1}{\frac{1}{2}\rho(V_1^2 - V_2^2)}$	diffusor efficiency
η_R	$\frac{P_2 - P_1}{\frac{1}{2}\rho(V_1^2 - V_2^2)}$	efficiency of ribbed wall diffusor
η_S	$\frac{P_2 - P_1}{\frac{1}{2}\rho(V_1^2 - V_2^2)}$	efficiency of smooth wall diffusor

CHAPTER I

INTRODUCTION

Much work has been done and many papers written concerning studies of diffusor performance. Most of these studies are limited to the study of diffusors operating with a total opening angle of less than 15 degrees. Cocanower, Kline, and Johnston, Ref. [1], have proposed a general theory for predicting diffusor performance for a variety of two and three dimensional diffusors. Their theory has been shown to be in good agreement with experimental tests.

The studies of diffusor performance for diffusors operating at large opening angles have not progressed as rapidly as the small angle diffusor work because of the complications associated with the severe turbulence resulting when flow separation occurs at the diffusor walls. This separation of flow is responsible for the large losses and poor performance normally associated with wide angle diffusors.

Two studies which deal with the problem of wide angle diffusors are the papers of Waitman, Reneau, and Kline, Ref. 2, and of Moore, Carl, and Kline, Ref. 3. Each of these studies deals with the conditions affecting flow separation in wide angle diffusors.

The flow separation phenomena observed and discussed by Moore, Carl, and Kline in connection with water table tests were also observed in the air flow tests of this investigation. These phenomena are discussed in Section 3.6 of Chapter III.

Migay, Ref. 4, noted an improvement in the efficiencies of diffusors operating at wide opening angles when transverse grooves were cut into the diverging walls. His explanation for this improvement in

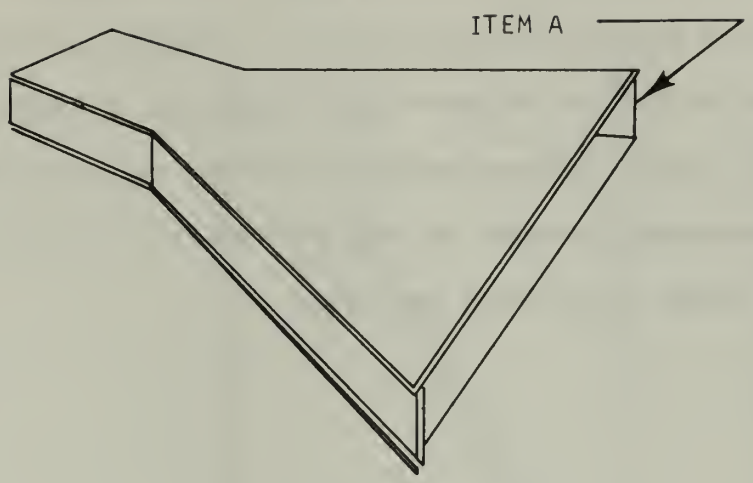
efficiency was that the "large separation" normally occurring without the grooves is replaced, because of their effect, by a series of "smaller separations." The resulting losses associated with these "smaller separations" are apparently less than the loss associated with the "large separation." The efficiency is thereby improved.

Migay cites the results of many tests which support his claim of an improved efficiency when operating with a grooved configuration. Unfortunately, many of the results cited are not adequately documented. The results of the two dimensional experimentation, for example, are presented as the ratio of ribbed wall diffusor efficiency to that of a smooth wall diffusor operating under the same conditions. No information is available concerning the specific conditions under which the tests were conducted, and the actual efficiencies of each of the diffusors are not presented in the paper.

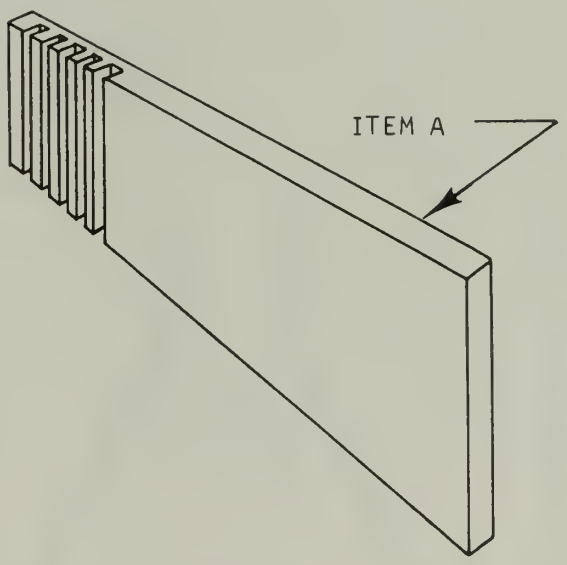
The over-all objective of this study was to determine experimentally the performance of a two dimensional ribbed wall diffusor. It was hoped that the optimum operating range of such a diffusor could be found and compared with a smooth walled diffusor operating under similar conditions.

Figure 1 illustrates the type of diffusor used for the experiment. The detailed insert in the figure shows what is meant by the term "ribbed wall."

Because of time limitations, the scope of this study was narrowed to the study of one particular rib configuration. The geometry of this configuration is discussed in Section 2.4 of Chapter II. A limited investigation was also made to determine the effect that varying the number of grooves had upon the performance of the ribbed wall diffusor.



TWO DIMENSIONAL DIFFUSOR



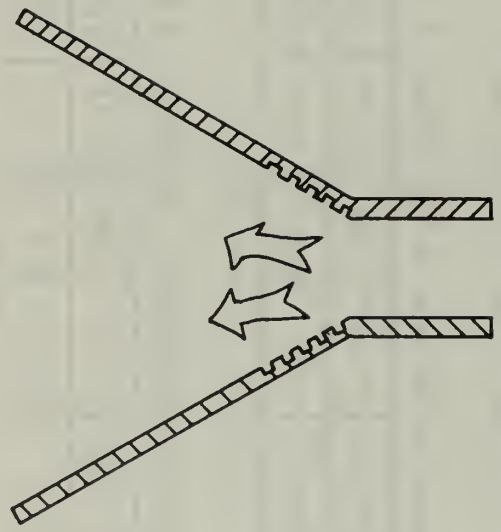
DETAIL OF RIBBED WALL CONFIGURATION

FIGURE 1

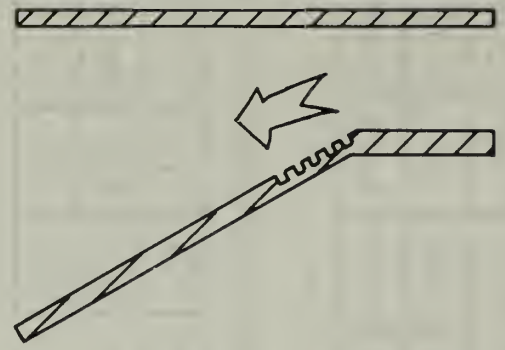
TWO DIMENSIONAL DIFFUSOR AND
DETAIL OF A RIBBED WALL
CONFIGURATION

Migay cites a limited amount of data related to a two dimensional ribbed wall diffusor. The data were obtained using a one sided diffusor with an asymmetric opening angle of 20 degrees. Figure 2 shows the type of diffusor used. Table I is a summary of the information presented in Ref. 4 related to two dimensional diffusors.

The initial rib configuration utilized for this study was chosen to be approximately equal to that used in Ref. 1. In this study, however, a symmetric diffusor was used.



SYMMETRIC TWO DIMENSIONAL DIFFUSOR



ASYMMETRIC TWO DIMENSIONAL DIFFUSOR

FIGURE 2

ILLUSTRATION OF AN ASYMMETRIC TWO DIMENSIONAL DIFFUSOR OF THE TYPE USED IN REF. 1 AND A SYMMETRIC TWO DIMENSIONAL DIFFUSOR OF THE TYPE USED IN THIS STUDY

TABLE I

SUMMARY OF TWO DIMENSIONAL DIFFUSOR STUDIES FROM REF. 1

Effect of Parameter A (B = 5mm)

	1.0	0.857	0.915	1.25	1.46	1.64	1.68	1.71	
A (mm)	0.0	0.500	1.000	2.00	4.00	8.00	10.0	15.0	
A/B	0.0	0.100	0.250	0.400	0.800	1.600	2.00	3.00	

Effect of Parameter B (A = 20mm)

	1.61	1.7	1.71		0.5	
B	1.0	3.0	5.0	unstab.	16	
A/B	20	6.7	4.0		1.25	

Effect of Number of Grooves N (B = 1mm, A = 20mm)

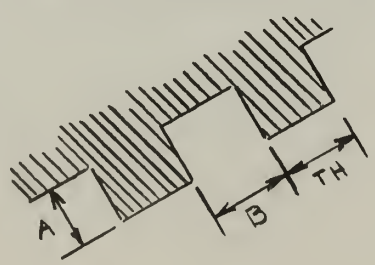
	1.04	1.13	1.30	1.515	1.63	1.68	1.71	1.71	1.71
N	1	2	3	4	5	6	7	10	15

Effect of Number of Grooves N (B = 3mm, A = 20mm)

	1.06	1.14	1.29	1.40	1.54	1.57	1.63	1.64	1.64
N	1	3	5	7	9	11	13	15	40

Effect of Number of Grooves N (B = 5mm, A = 20mm)

	0.6	0.7	0.78	1.5	1.68	1.71	1.71		
N	1	2	3	4	5	6	15		



CHAPTER II

EXPERIMENTAL PROCEDURES

2.1 Experimental set-up. The equipment used for this study was located in the "New Addition" of Building 230 at the Jet Propulsion Laboratories, Naval Postgraduate School, Monterey, California. Figure 3 is a schematic of the installation. The source of air for the tests was the Carrier Air Compressor installed in Building 230.

2.2 Pressure readings. All pressure measurements in the flow field were made using a Fused Quartz Precision Pressure Gauge manufactured by Texas Instruments Inc. of Houston, Texas. Prior to, and twice during the time period of the tests, the pressure instrument was calibrated using a water manometer. The calibration remained invariant throughout the duration of the test; and the value of 0.8 inches of water pressure per increment, or count, on the instrument was used as the conversion coefficient for all pressure measurements. The details of the conversion of the pressure and temperature readings are discussed in Chapter III, Sections 3.1 and 3.2.

Atmospheric pressures were read from a standard wall barometer. Two pressure readings were required at the flow nozzle. The static pressure upstream, P_u, and the drop in static pressure across the nozzle, ΔP, were measured and recorded for the purpose of determining the flow rate through the system. The computations involved in the determination of the flow rate are discussed in Chapter III, Section 3.3.

Two pressures were measured at the inlet plane of the diffusor, the static pressure and the dynamic head, q_1. The static pressure

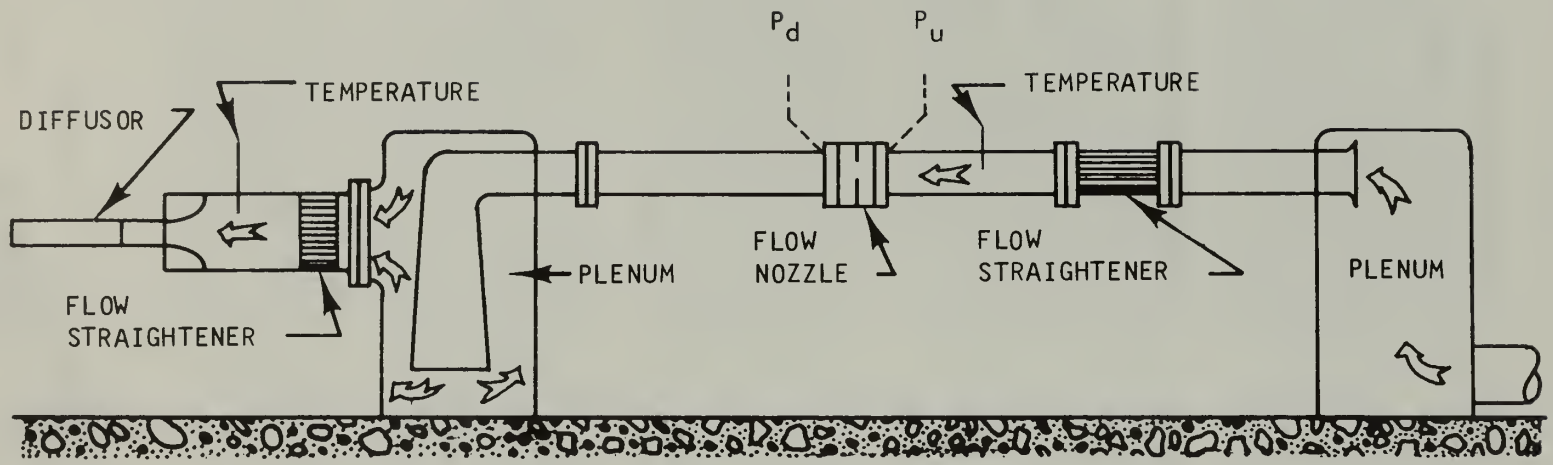


FIGURE 3

SCHEMATIC OF THE EXPERIMENTAL INSTALLATION HOUSED IN THE "NEW ADDITION"
OF BUILDING 230, JET PROPULSION LABORATORY, NPGS, MONTEREY

was assumed to be uniform in the plane of the throat. Two static taps were located at the top of the diffusor inlet and two at the bottom. All four of these static pressure taps were connected to the pressure measuring instrument through a common lead. The total pressure was measured at three positions in the central region of the flow, free of the boundary layer effect. Figure 4 shows the location of the pressure orifices and the details of the total pressure probe construction. The probe was manufactured by Mr. M. O dell, machinist, Aeronautics Department, NPGS.

Figure 5 is a schematic of the pressure instrument hook-up. By opening and closing various pairs of the six switches, it was possible to measure all of the required pressures.

Section 3.4 of Chapter III illustrates how the conditions at the throat were calculated using these pressure measurements.

2.3 Temperature measurements. Two total temperature readings were taken in the flow field. The first was taken just ahead of the flow nozzle and was used in the flow rate calculation. The second total temperature measurement was taken just ahead of the diffusor inlet. This temperature was used in the determination of the flow conditions at the inlet.

All flow field temperatures were measured using a thermocouple. Section 3.1 of Chapter III discusses the details of the temperature reading conversions. The ambient air temperatures were measured with ordinary mercury bulb thermometers.

2.4 Measuring and recording the data. The rate of flow through the system was regulated by bleeding the compressor output to the

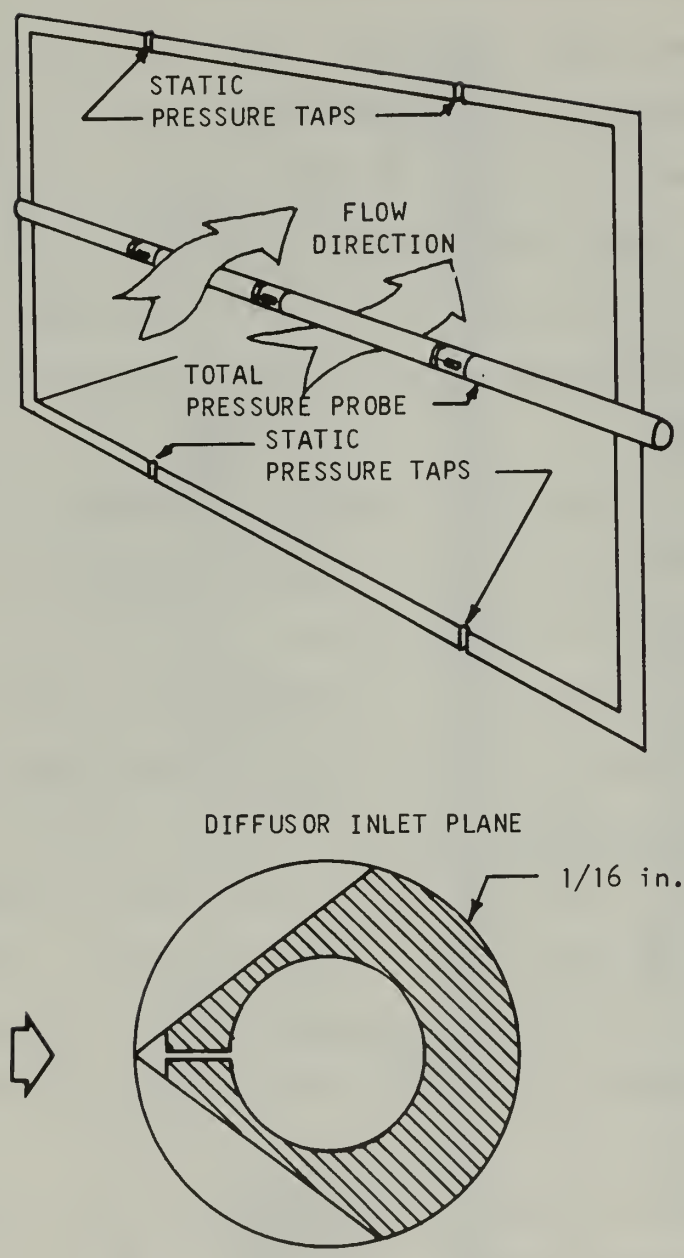


FIGURE 4

SCHEMATIC OF THE DIFFUSOR INLET PLANE ILLUSTRATING THE LOCATION OF THE TOTAL AND STATIC PRESSURE TAPS

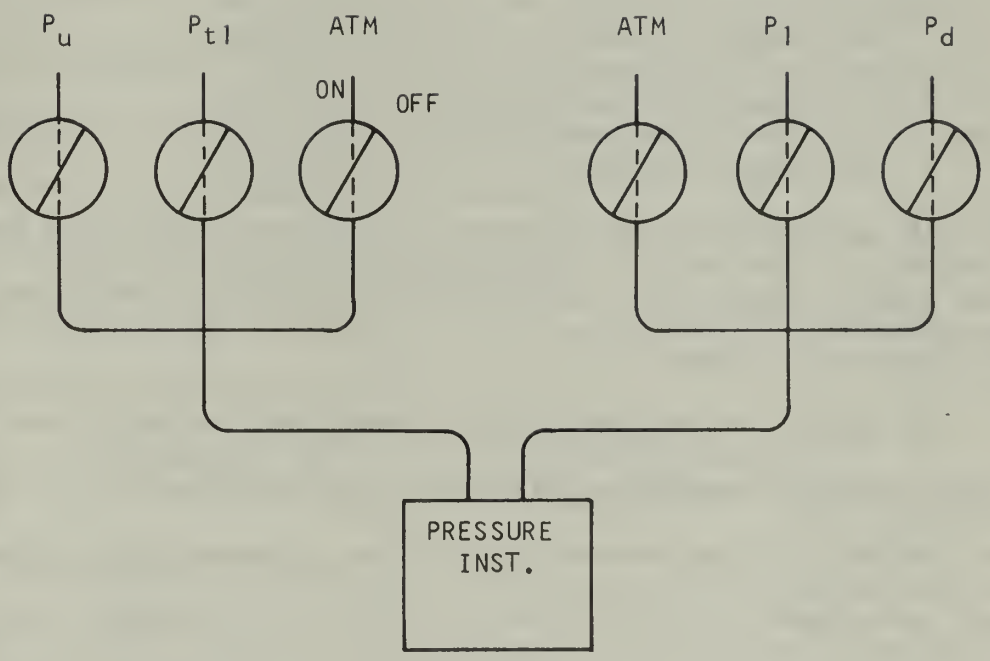


FIGURE 5

SCHEMATIC OF THE PRESSURE INSTRUMENTATION INSTALLATION

atmosphere. The maximum obtainable flow rate was approximately 2.4 lb_m/sec. At this flow rate, the velocity in the center of the inlet flow channel was approximately 210 ft/sec.

In the initial phase of the experiment tests were made at diffusor angles varying from $\beta = 10^o$ to $\beta = 60^o$. At each angle, the flow rate was varied between the maximum of 2.4 and a minimum of 0.8 lb_m/sec.

Tests were made at each of the angles with smooth walls and with ribbed walls configured as indicated below:

N: number of grooves = 10

b: width of grooves = 0.125 in.

t: spacing between grooves = 0.060 in.

a: depth of grooves = 0.700 in.

This rib configuration was chosen as a close approximation to the rib sizes used by Migay in the two dimensional diffusor study cited earlier and summarized in Table I.

The results of this phase of the experiment indicated that the ribbed walls performed best, relative to the smooth walls, at $\beta = 32^o$ and a velocity of approximately 155 ft/sec. Consequently, further tests were conducted at this operating point in an attempt to determine how the performance varied as a function of the number of grooves. In this phase of the experiment the number of grooves was increased by one for each successive run. The results of these tests are discussed in Chapter IV.

The program used to perform the required calculations is discussed in detail in Appendix A. A sample data sheet, a list of the variable names used on the sample data sheet, and a listing of input variables are included with the discussion of the program.

CHAPTER III

COMPUTATIONS AND ANALYSIS

3.1 Temperature measurement conversions. The thermocouple readings, recorded in millivolts, were converted to degrees Fahrenheit by the following equation:

$$°F = 32 + 35.98(mv) - .435(mv)^2 \qquad (3\text{-}1)$$

This equation is a least squares fit of the values for conversion from millivolts to degrees Fahrenheit as specified in the National Bureau of Standards Circular 561 for iron constantan thermocouples. Equation (3-1) is valid only if the reference junction is maintained at a temperature of 32 degrees Fahrenheit.

3.2 Pressure measurement conversions. The barometric pressure, measured and recorded in inches of mercury, was converted to pounds per square inch by using the following equation:

$$P = .4912\, P\left[1 - \frac{.0001634\ t}{1 + .0001818\ t}\right] \qquad (3\text{-}2)$$

The two coefficients multiplying t, the temperature in degrees centigrade, are thermal expansion coefficients for the mercury in the barometer and the brass upon which the scale of the barometer is engraved. The factor .4912 is the conversion factor for converting pressure measured in units of inches of mercury to units of lbs. per sq. in. Equation (3-1), the conversion factor, and the correction coefficients were obtained from Ref. 5, pages 1-157.

3.3 Flow rate measurements. References 6 and 7 provide general methods, procedures, and calculations concerning flow rate measurements

using flow metering orifices and nozzles. The flow metering nozzle used to determine the flow rate for these tests was constructed in accordance with the specifications of Ref. 8. A nozzle was selected, rather than a square-edged orifice, because the calculations were felt to be more easily adaptable to computerized methods.

From Ref. 8, page 5, Eq. (1a), slightly modified, the flow rate through the flow metering nozzle in lb_m/sec is:

$$\dot{w} = \alpha \varepsilon A_d f_t f_r \sqrt{2 g_c \delta_u (P_u - P_d)} \tag{3-3}$$

The quantities in Eq. (3-3) are identified below:

$\dot{w}$ flow rate (lb_m/sec)

α discharge coefficient

ε density coefficient

A_d area of nozzle opening ($in.^2$)

f_t area multiplier

f_r Reynolds number correction

g_c conversion factor (32.17 ft. $lb_m/sec^2 lb_f$)

$(P_u - P_d)$ pressure drop across nozzle (psi)

δ_u upstream "density" (non-standard units)

By assuming the flow to be a perfect gas, δ_u can be expressed as a function of the temperature, Tu.

$$\delta_u = \frac{P_u}{R_g T_u} \tag{3-4}$$

R_g gas constant for air ($53.35 \frac{ft \cdot lb_f}{lb_m \, ^\circ R}$)

T_u temperature upstream ($^\circ R$)

The "equivalent flow rate," denoted as $\dot{w}^*$, and defined by Eq. (3-5), provided a computational means of determining the flow rate.

$$\overset{*}{W} = \frac{\dot{W}\sqrt{T_u}}{P_u}\sqrt{\frac{R_g}{g_c}} \qquad (3\text{-}5)$$

In Eq. (3-5), $\overset{*}{W}$ has the units of $in.^2$.

After substituting for $\dot{W}$ and ρ_u Eq. (3-5) becomes:

$$\overset{*}{W} = \alpha \varepsilon A_d f_t f_r \sqrt{2}\sqrt{\frac{P_u - P_d}{P_u}} \qquad (3\text{-}6)$$

The table below lists the values of the coefficients in Eq. (3-6) which are applicable to the particular nozzle installed for these tests.

TABLE II

SUMMARY OF FLOW RATE CALCULATION COEFFICIENTS

Coefficient Symbol	Coefficient Value	Source of Value
α	1.114	Ref. 4
ε	Eq. (3-7)	Ref. 2
f_t	Eq. (3-8)	Ref. 2
f_r	1.0	Ref. 4
A_d	7.1728	πr^2

If $X = \frac{P_u - P_d}{P_u}$, then the coefficient ε can be expressed by the equation,

$$\varepsilon = \sqrt{2.433\ \frac{(1-X)^{1.428}}{X}\ \frac{1-(1-X)^{.286}}{1-.305(1-X)^{1.428}}} \qquad (3\text{-}7)$$

If t_u is the temperature of the flow upstream of the nozzle, expressed in degrees Fahrenheit, then the coefficient f_t is given by the equation,

$$f_t = 1 + .0015\left(\frac{t_u - 60}{100}\right) \qquad (3\text{-}8)$$

Equation (3-6) may be greatly simplified by combining all of the known constant coefficients into one constant, c.

$$C = \alpha f_r A_d \sqrt{2} = 11.30 \text{ in.}^2$$

Thus, Eq. (3-6) becomes:

$$\overset{*}{W} = 11.30\, \varepsilon f_t \sqrt{\frac{(P_u - P_d)}{P_u}} \tag{3-9}$$

Finally, the mass flow rate can be calculated by:

$$\dot{W} = \overset{*}{W} \frac{P_u}{\sqrt{T_u}} \sqrt{\frac{g_c}{R_g}} \tag{3-10}$$

3.4 Flow conditions at the diffusor inlet. Velocity and total pressure measurements across the inlet of the diffusor indicated that the static pressure was uniform throughout the inlet plane. It was assumed that the total pressure at the inlet was constant in the region outside of the boundary layer. Based upon this assumption, the Mach number in the central region of the flow at the inlet was determined by solving the following isentropic relationship for M_1:

$$\frac{P_{t_1}}{P_1} = \left(1 + \frac{\gamma - 1}{2} M_1^2\right)^{\frac{\gamma}{\gamma - 1}} \tag{3-11}$$

The measured values of P_1 and P_{t1} were used to determine M_1.

$$M_1 = \left\{ \frac{2}{\gamma - 1} \left[\left(\frac{P_{t1}}{P_1} \right)^{\frac{\gamma - 1}{\gamma}} - 1 \right] \right\} \tag{3-12}$$

The static temperature at the inlet was determined by using the previously determined Mach number and the following equation:

$$\frac{T_{t1}}{T_1} = \left(1 + \frac{\gamma - 1}{2} M_1^2\right) \tag{3-13}$$

Solving Eq. (3-13) for T_1 yields the required relationship:

$$T_1 = \frac{T_{t1}}{1 + \frac{\gamma - 1}{2} M_1^2} \tag{3-14}$$

Once T_1, the static temperature, was determined, it was possible to evaluate a, the speed of sound, and subsequently the midstream velocity at the inlet.

$$V_{max} = M_1 a_1 = M_1 \sqrt{\gamma R_g g_c T_1} \tag{3-15}$$

The velocity in the central region of the flow is indicated by V_{max}.

By assuming the flow to be a perfect gas, enough information was available to calculate the density of the flow at the inlet. It was assumed that the density remained constant across the inlet plane.

$$\rho_1 = \frac{P_1 \times 144}{R_g g_c T_1} \tag{3-16}$$

Equation (3-16) expresses the density in units of slugs/ft^3.

The Reynolds number based upon the equivalent diameter of the inlet was determined by expressing the kinematic viscosity of air as a function of temperature. The expression represents a fit of the data tabulated on page 8 of Ref. 9. The following expression is considered valid only for the temperature range of 50°F. to 104°F:

$$\nu_1 = (0.6\, t_1 + 120) \times 10^{-6} \tag{3-17}$$

The units of ν are ft^2/sec.

3.5 Integrated flow rate at the diffusor inlet. All of the calculations related to the conditions at the inlet and the performance of the diffusor were dependent upon the total pressure, static pressure, and total temperature measurements at the diffusor inlet. It was felt

that some method of evaluating the reliability of these measurements should be incorporated into the computational procedures. The method decided upon was to compare the flow rate at the inlet, computed from the velocity and density as determined from these measurements, against the flow rate measured at the flow nozzle. Since the two flow rates were determined from completely independent measurements, it was felt that any erroneous readings, or errors in recording the data, would become apparent when the two flow rates were compared.

Prior to performing the calculations to determine the flow rate through the diffusor, tests were made with a hot wire anemometer to determine the velocity profiles at the inlet. Figure 6 is the velocity ratio, V/V_{max}, plotted as a function of the distance, h, from the surface of the wall. V_{max} is the velocity in the central region of the flow. Figure 7 represents the same velocity ratio as measured from the side wall. The profiles represented in Figs. 6 and 7 were measured at the mid-span position of the top and side walls respectively.

In each instance, it was possible to find analytic expressions which closely approximated the velocity profiles. The data plotted were taken at several velocities representative of all anticipated operating conditions. Although it was recognized that the velocity profiles vary as a function of velocity, tests indicated that the variation was minor and under the anticipated velocity operating range would not exceed the variations caused solely by instrumentation error. The total change in the flow rate determination over the extremes in the velocity profile predictions was found to be a fraction of 1 per cent of the total flow rate.

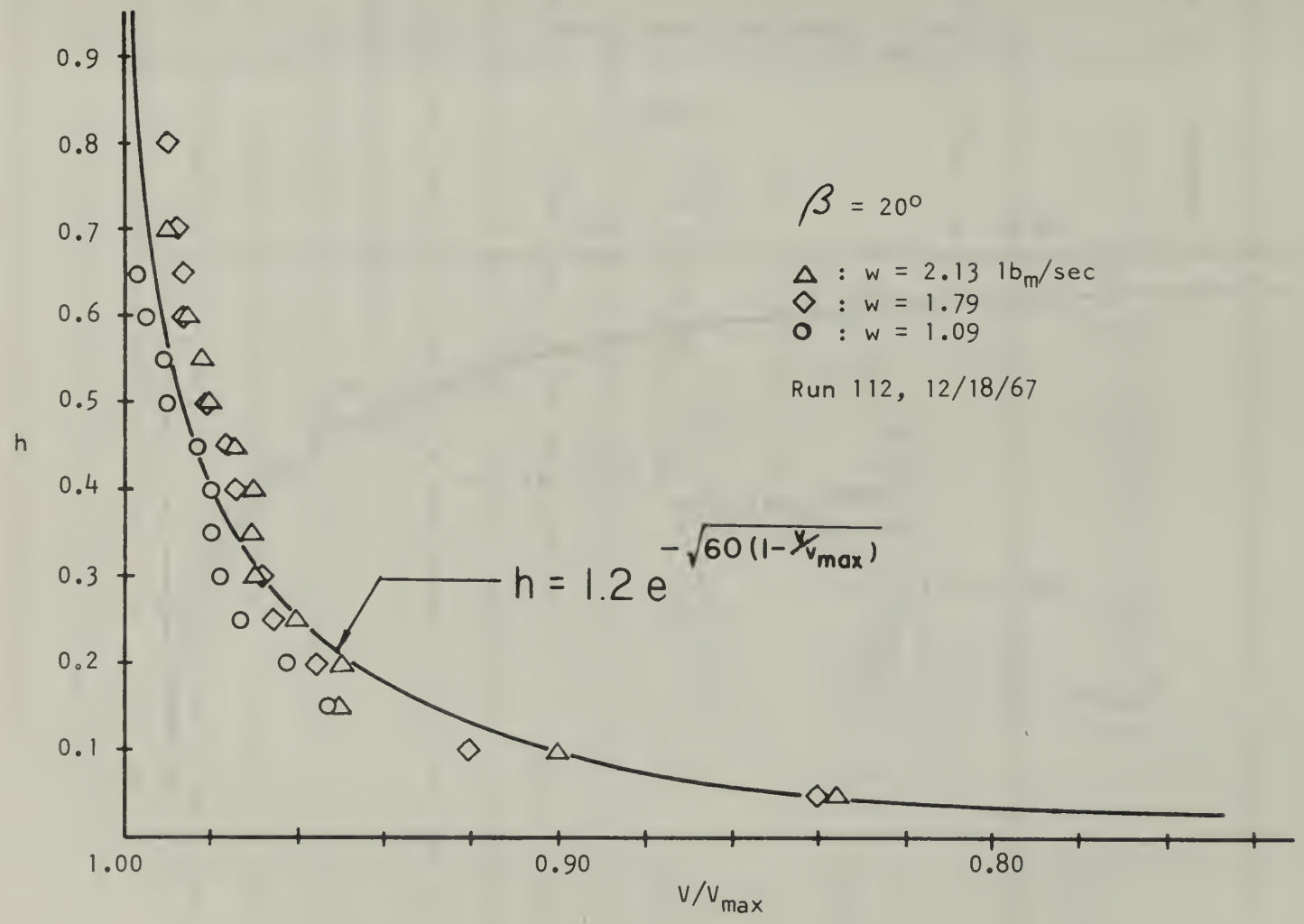


FIGURE 6

DIFFUSOR INLET VELOCITY PROFILE AT MID-SPAN OF TOP WALL WITH EXPONENTIAL EXPRESSION USED TO APPROXIMATE THE SHAPE OF PROFILE

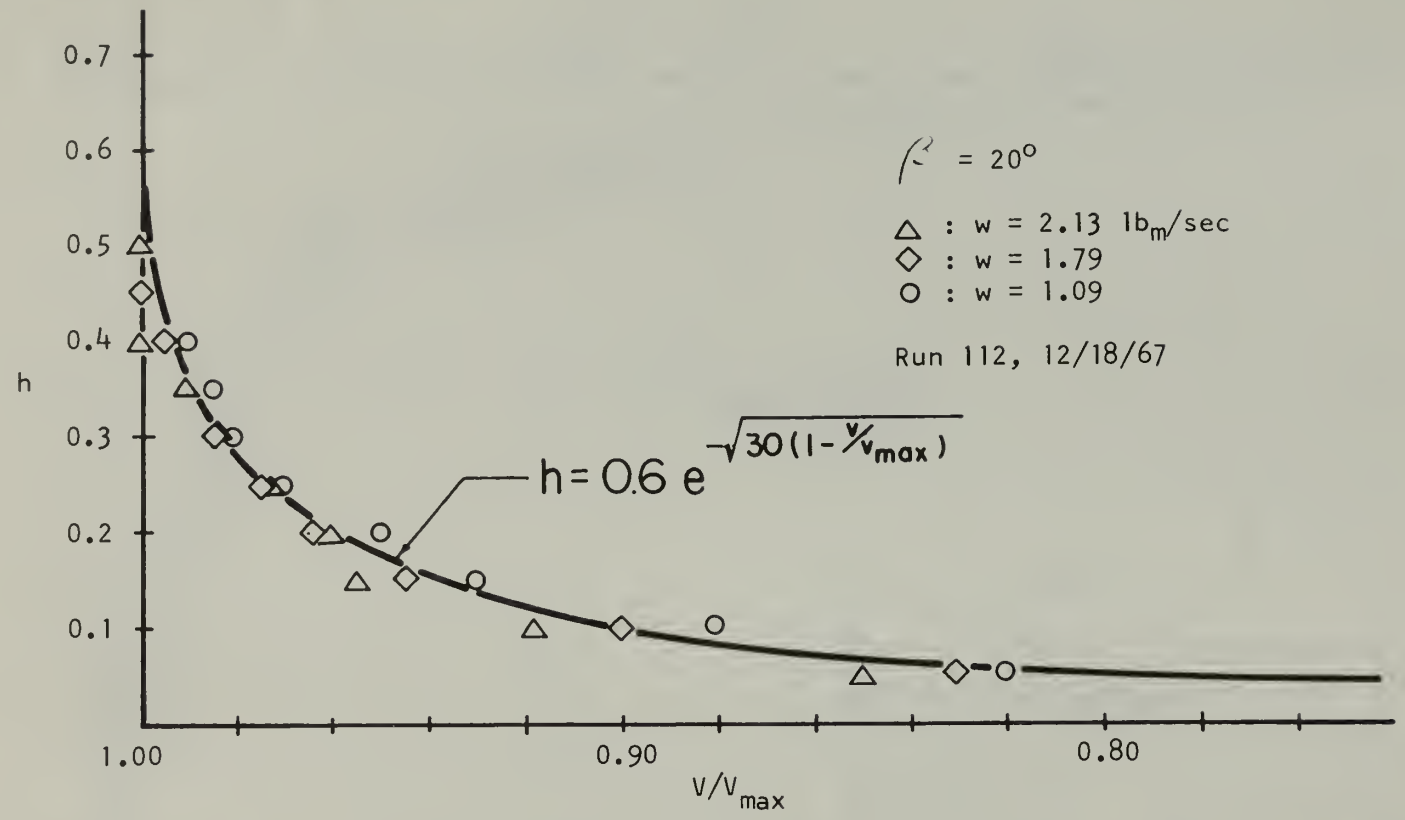


FIGURE 7

DIFFUSOR INLET VELOCITY PROFILE AT MID-SPAN OF SIDE WALL WITH EXPONENTIAL EXPRESSION USED TO APPROXIMATE THE SHAPE OF PROFILE

The expression used to approximate the velocity along the top wall is:

$$h = 1.20\, e^{-\sqrt{60(1 - V/V_{max})}} \tag{3-18}$$

When solved for V as a function of h, the distance from the wall, Eq. (3-18) becomes:

$$V = V_{max}\left\{1 - \frac{1}{60}\left(\ln \frac{1.20}{h}\right)^2\right\} \tag{3-19}$$

A similar expression was obtained for the shape of the velocity profile at the side wall.

$$h = 0.60\, e^{-\sqrt{30(1 - V/V_{max})}} \tag{3-20}$$

Solving for V as a function of h yields:

$$V = V_{max}\left\{1 - \frac{1}{30}\left(\ln \frac{0.60}{h}\right)^2\right\} \tag{3-21}$$

Figure 8 is a cross-sectional view of the inlet plane. The region labeled "C" is the area outside of the effect of the boundary layer. It was assumed that the velocity in this region, previously referred to as V_{max}, was constant throughout. Measurements indicated that this assumption was reasonable.

A turbulence survey was made in the central region by feeding the hot wire anemometer output to an oscilloscope. The results of this study indicated that the 1 maximum velocity perturbation was less than 1 per cent of the mean velocity, V_{max}.

The regions labeled "F" and "D" in Fig. 8 represent those regions within the boundary layer along the top, bottom, and side walls respectively.

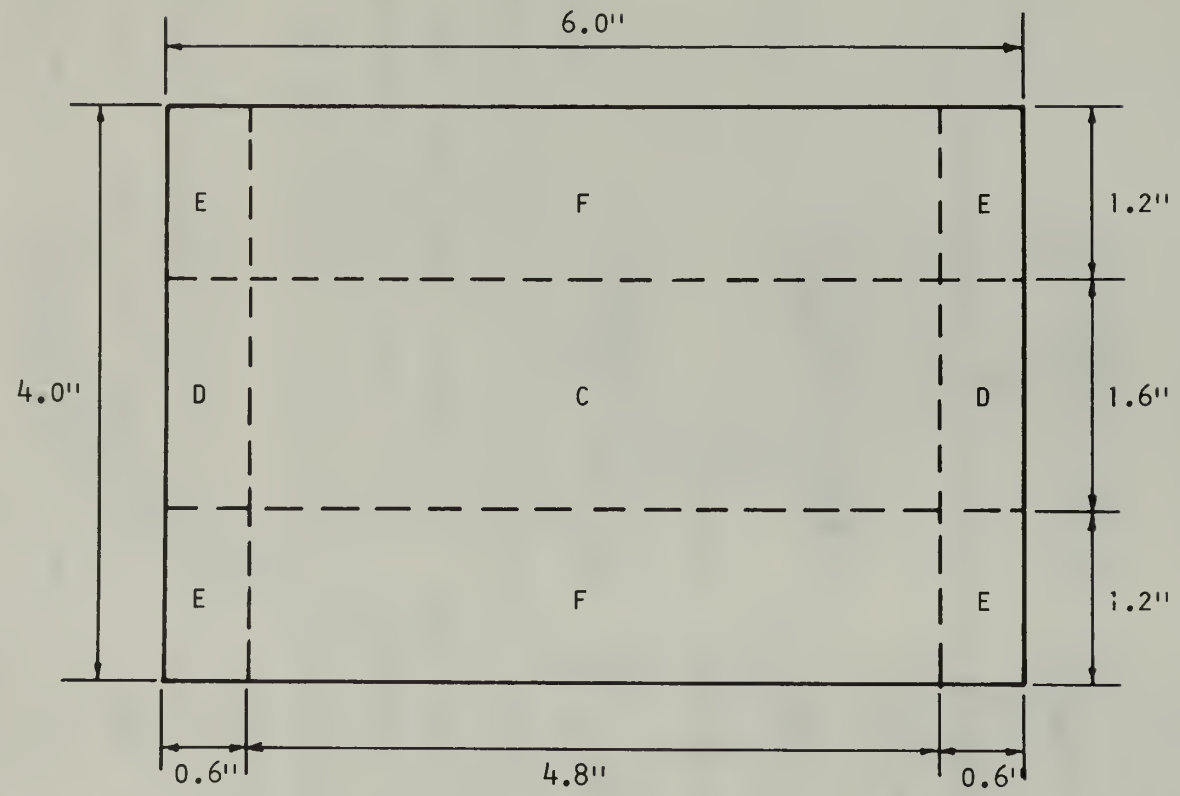


FIGURE 8

INLET PLANE OF DIFFUSOR SHOWING THE LOCATION OF BOUNDARY LAYERS AND FLOW REGIONS AS USED IN THE DETERMINATION OF THE FLOW RATE THROUGH THE INLET

Although it was not possible to accurately measure the velocity profiles on the bottom and opposite side wall, those measurements taken indicated that the variations from wall to wall and top to bottom were slight. Thus, it was assumed that the velocity profiles on opposite walls were identical.

The corners, indicated as "E" in Fig. 8, were assumed to have a velocity distribution equal to the product of the V/V_{max} ratios from each wall as a function of the respective distances. Figure 9 shows how this was done. The velocity assumed to exist at the point p, indicated in Fig. 9, was assumed to be the product of the velocity ratio V/V_{max}, given by Eq. (3-19) for the distance h_1, from the top wall and the velocity ratio V/V_{max}, given by Eq. (3-20), for the specified distance, h_2, from the side wall.

The diagonal line indicated as "corner survey path line" in Fig. 9 is the line upon which a survey of velocities was made. Figure 10 shows the comparison between what the above assumption predicted for the velocities along the line and the actual measured values of V/V_{max}. The analytic expression for the velocity at any point in the corner region is given as a function of the two distances h_1 and h_2.

$$V = V_{max}\left\{1-\frac{1}{60}\left(\ln\frac{1.2}{h_1}\right)^2\right\}\left\{1-\frac{1}{30}\left(\ln\frac{0.6}{h_2}\right)^2\right\} \qquad (3\text{-}22)$$

The purpose of this investigation into the velocity profile at the inlet was to obtain a measure of the reliability, or validity, of the pressure readings. This was accomplished by using the measured values of the velocity and density together with the estimates of the velocity profile to integrate across the inlet and determine the flow rate.

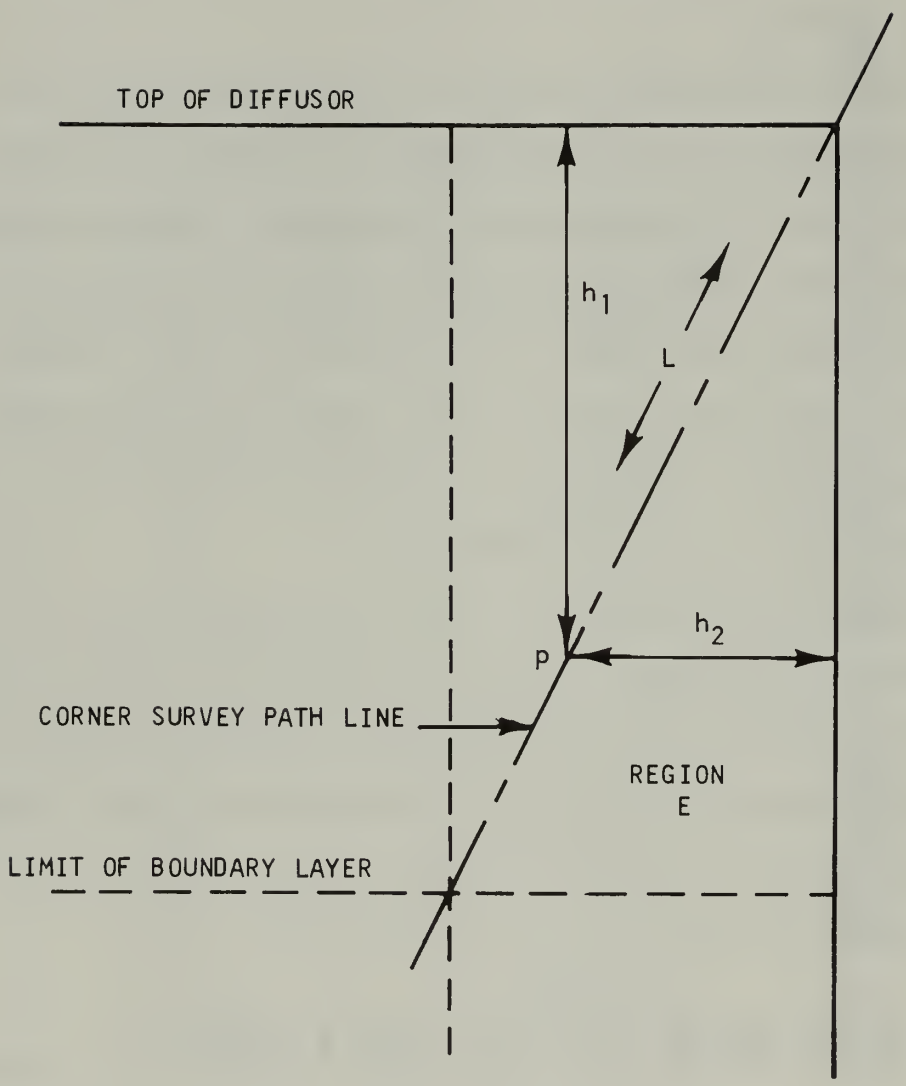


FIGURE 9

THE CORNER REGION (E) OF THE INLET PLANE

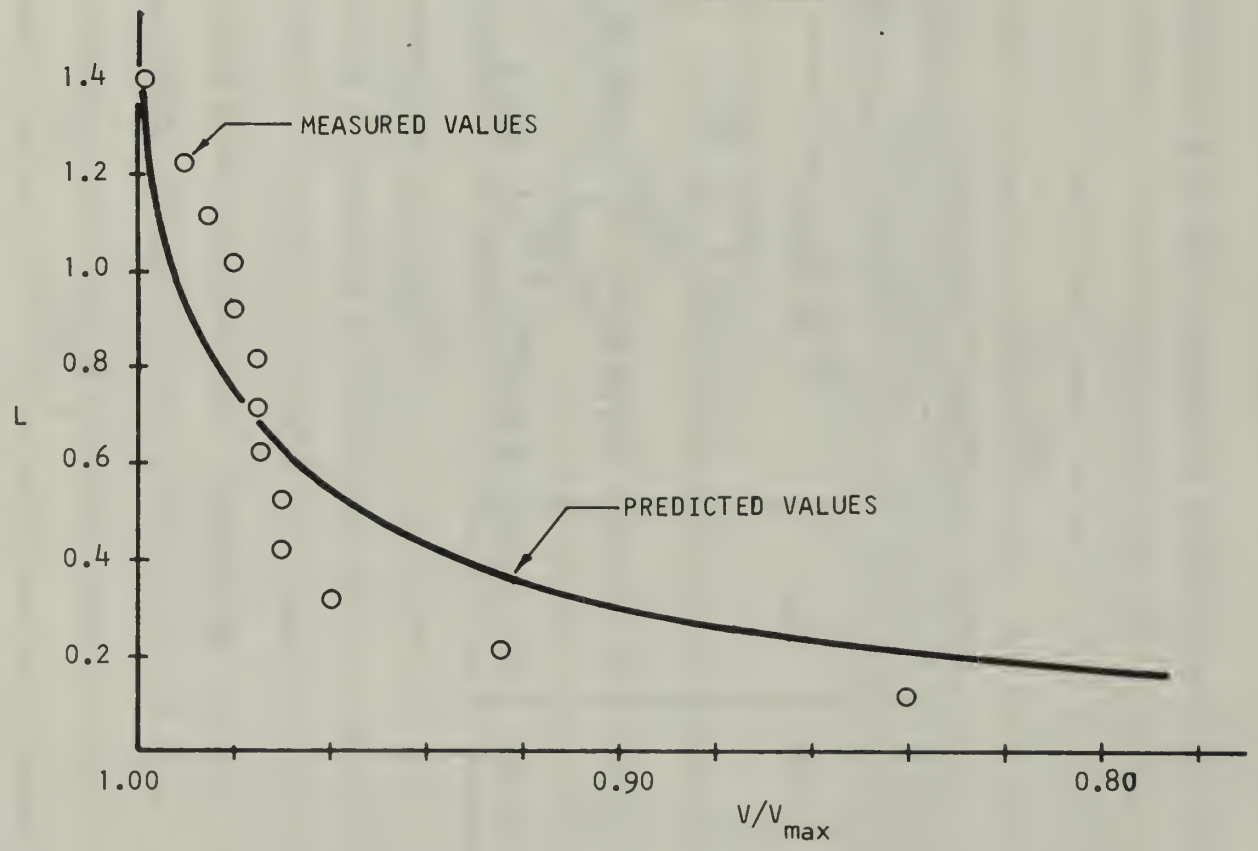


FIGURE 10

MEASURED AND PREDICTED VELOCITIES ALONG THE CORNER SURVEY PATH LINE

The calculation for the mass flow rate is expressed by the following equation when the flow is considered to be incompressible:

$$\dot{w} = \rho g_c L \int_0^H V \, dh \qquad (3\text{-}23)$$

Table III is a breakdown of the mass flow rate calculations for each of the regions specified in Fig. 9.

TABLE III

SUMMARY OF CONTINUITY CALCULATIONS

Region	Area	Velocity	Mass Flow (lb_m/sec)	Eq.
C	0.008	V_{max}	$\rho g_c V_{max} A$	(3-24)
D	0.013	Eq. (3-19)	$0.022 \rho g_c \int_0^{0.6} V_1 \, dh_1$	(3-25)
E	0.020	Eq. (3-22)	$0.028 \rho g_c \int_0^{1.2} \int_0^{0.6} V_{1,2} \, dh_1 dh_2$	(3-26)
F	0.080	Eq. (3-21)	$0.067 \rho g_c \int_0^{1.2} V_2 \, dh_2$	(3-27)

The flow rate determined by this integration was compared to the flow rate measured at the flow nozzle as discussed in Section 3.2. In general, the agreement was within 1 per cent.

3.6 Diffusor performance. The conditions which existed at the diffusor inlet were found to be generally steady, and the measurements were felt to be reliable indicators of the flow at that plane. It was found, however, that conditions at the exit plane were, under most operating conditions, extremely turbulent. For large opening angles, of particular interest in this study, the flow actually reversed direction along the diffusor walls after separation had occurred. Moreover, at opening angles greater than 26 degrees, the flow was unsteady in that

it would separate first on one side of the diffusor and then on the other. It was noted that under certain conditions the flow could be directed along one wall of the diffusor while complete separation existed along the opposite wall. The flow could then be shifted to the opposite wall causing the separation to shift sides. It was also noted that the diffusor could be made to separate at both sides simultaneously causing a "free jet" flow straight out of the inlet throat.

Because of these non-uniform conditions which existed at the exit, it was not possible to measure a single meaningful exit velocity. The only flow condition which could be accurately measured at the exit was the static pressure, P_2. Because the diffusor exhausted to atmospheric conditions at subsonic velocities, the exit static pressure was taken to be equal to atmospheric pressure.

Not being able to measure an exit velocity posed a serious problem in attempting to measure diffusor performance. Most definitions of diffusor efficiency, for example, require a knowledge of the exit velocity, V_2. Migay, Ref. 1, defines diffusor efficiency as:

$$\eta_D = \frac{P_2 - P_1}{\frac{1}{2}\rho(V_1^2 - V_2^2)} \qquad (3\text{-}28)$$

He makes no attempt to explain the meaning of V_2 or how it was obtained.

A more convenient and perhaps realistic criteria for diffusor performance are the coefficient of pressure recovery, defined as

$$C_{PR} = \frac{P_2 - P_1}{\frac{1}{2}\rho V_1^2} \qquad (3\text{-}29)$$

This measure of diffusor performance has the distinct advantage that all of the quantities can be easily determined. V_{max}, the velocity of the flow in "Region C," Fig. 8, was chosen as the reference velocity V_1, to be used in Eq. (3-29).

In order to compare the results of this test with those published in Ref. 1, some scheme had to be decided upon to produce a quantity V_2 for Eq. (3-28). One method used was simply to assume that the central flow at the inlet, with velocity V_{max}, was expanded completely and incompressibly from area A_1 to area A_2. V_2 is an ideal expansion of the midstream velocity at the inlet.

A second means of evaluating the efficiency was to determine the ratio of the measured to the ideal coefficient of pressure recovery.

The ideal coefficient of pressure recovery can be expressed as a function of the inlet and exit areas,

$$C_{PR_i} = 1 - \left(\frac{A_1}{A_2}\right)^2 \qquad (3\text{-}30)$$

Equation (3-30) was derived by substituting Bernouilli's equation and the equation of continuity for incompressible flow into Eq. (3-29).

3.7 Measurement reliability indicator. In order to obtain another indication of the reliability of the pressure and temperature measurements at the diffusor inlet, a comparison was made of the measured flow rate based upon the flow metering nozzle and the flow rate calculated by integrating the velocity over the area of the diffusor inlet as described in Section 3.4. The quantity referred to as the "data reliability indicator" was defined by the equation:

$$ERR = 1 - \frac{\dot{W}_{Noz}}{\dot{W}_{inlet}} \qquad (3\text{-}31)$$

CHAPTER IV

RESULTS AND RECOMMENDATIONS

4.1 Results. This project was conducted in three phases. The preliminary phase consisted of planning, building and evaluating the test equipment. The second phase consisted of the development of procedures and data reduction calculations. The final phase encompassed the testing required to determine the most desirable operating range for conducting further tests and an investigation to determine the effect of the number of grooves upon the ribbed wall diffusor performance. The results of each of these phases of the project are discussed individually in the following sections.

4.1.1 Preliminary phase. The comparison of the flow rate measured at the nozzle and the flow rate computed at the diffusor inlet provided a cross check of the pressure readings and the computed values of the Mach number and velocity. The data reliability indicator defined by Eq. (3-31) reflected the comparison of these two flow rates. The average value of this indicator for the last 50 data points recorded during the project was 0.0044. This indicates that the agreement was, on the average, within 0.5 per cent. This is comparable with the accuracy of the flow nozzle which is $\pm$ 0.5 per cent.

Section 3.6 of chapter III discusses the two methods used to determine the diffusor efficiency. It can be shown that the ratio C_{PR}/C_{PR_i} is identical to the efficiency defined by Eq. (3-28). Both methods of determining the efficiency were included in the calculations dealing with diffusor performance since Eq. (3-28) is based upon the calculated value of the density, ρ_1, whereas the ratio of pressure

recovery coefficients does not depend upon P_1. The comparison of these two efficiencies provided, therefore, an indication of the reliability of the measured value of the temperature and pressures at the inlet.

The third indication of the reliability of the test equipment and procedures was the repeatability of the tests. Table IV shows the results of tests run on separate days under similar operating conditions. It was felt that the repeatability indicated in Table IV was reasonably good and that a realistic performance determination could be made on the basis of these tests.

The results of the tests seemed to indicate that the test equipment and procedures could be relied upon to an extent consistent with the intended use of the calculated results. It was felt that sufficient safeguards had been incorporated into the computational system to provide adequate warning indications in the event that erroneous data were being processed.

4.1.2 Determination of the most desirable operating range. To accomplish the objective of this phase of the study, ribbed wall and smooth wall tests were run over a wide range of operating conditions.

Table V summarizes the results of this phase of the tests. Although runs were made from $\beta = 10^{\circ}$ to $\beta = 60^{\circ}$ for velocities ranging from 65 ft/sec to 210 ft/sec, only those values of β which were of particular interest to this study are presented in Table IV.

Figure 11 illustrates the operating range of particular interest for ribbed wall investigations. Figure 12 shows how the ribbed wall efficiency compares to that of the smooth wall diffusor in this region.

TABLE IV

RESULTS OF REPETITIVE TESTS UNDER SIMILAR OPERATING CONDITIONS

β	Ribbed Wall		Smooth Wall	
	Run No.	η_R	Run No.	η_S
26°	219	61.75	220	65.30
26°	221	62.86	202	66.53
28°	219	59.63	220	58.58
28°	221	59.68	---	-----
30°	219	58.94	220	53.51
30°	221	59.17	204	53.60
32°	219	56.96	220	47.84
32°	221	57.36	207	47.17

TABLE V

COMPARISON OF SMOOTH WALL AND RIBBED WALL DIFFUSOR EFFICIENCIES*

β	η_S	η_R	η_R/η_S
20°	83.06	-----	------
22°	81.21	78.29	0.9640
24°	-----	69.79	------
26°	65.30	61.75	0.9456
28°	58.58	59.63	1.0179
30°	53.51	58.44	1.1015
32°	47.84	56.95	1.1906
34°	43.51	34.55	0.7941
36°	39.30	29.82	0.7588
38°	34.55	-----	------
40°	31.66	27.69	0.8746

*All data recorded at a measured flow rate of approximately 1.78 lb_m/sec. Ribbed wall configuration:

A = 0.7 in.

B = 0.125 in.

TH = 0,06

N = 10

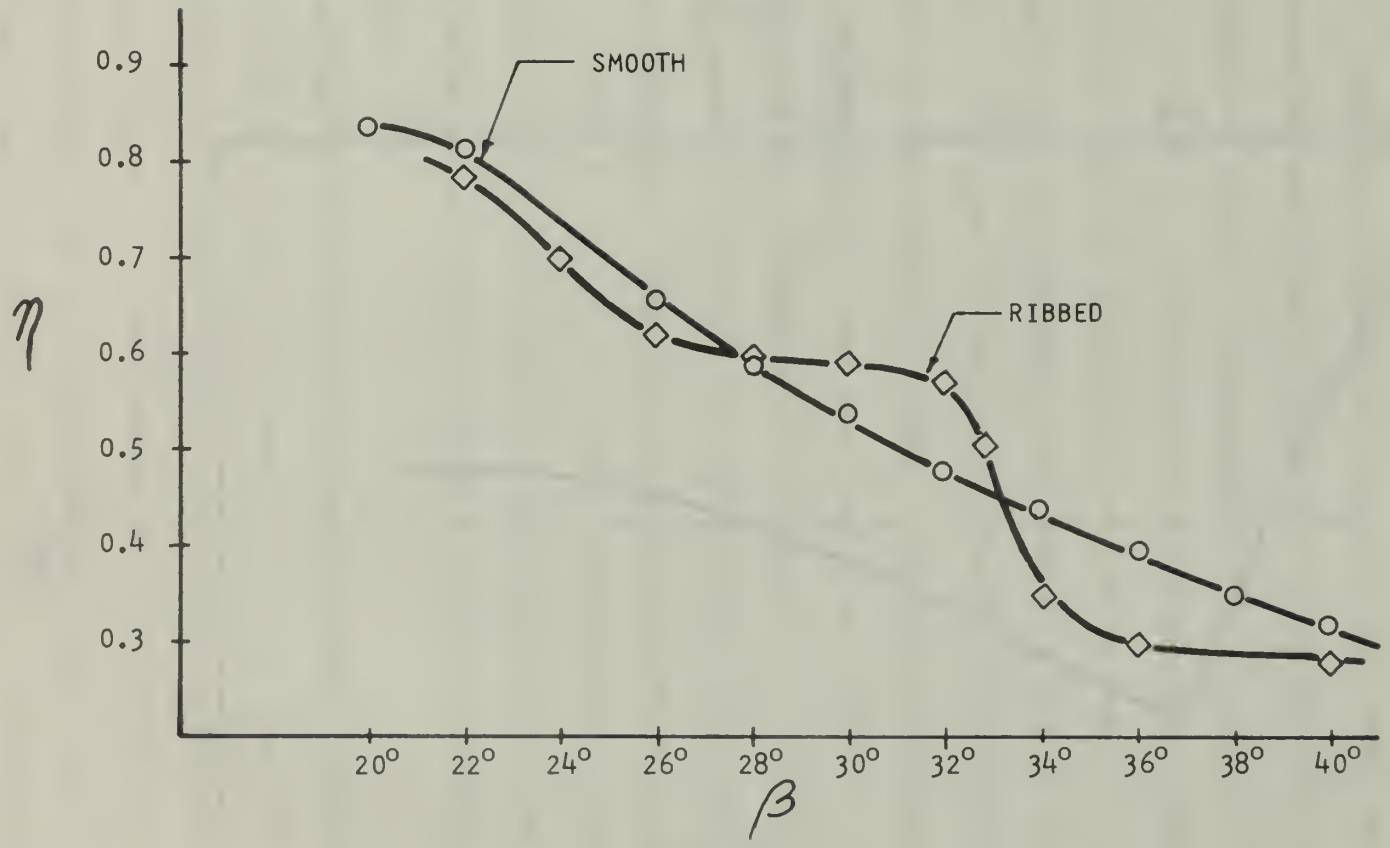


FIGURE 11

SUMMARY OF RIBBED WALL AND SMOOTH WALL DIFFUSOR EFFICIENCIES

TABLE V

COMPARISON OF SMOOTH WALL AND RIBBED WALL DIFFUSOR EFFICIENCIES*

β	η_S	η_R	η_R/η_S
20°	83.06	-----	------
22°	81.21	78.29	0.9640
24°	-----	69.79	------
26°	65.30	61.75	0.9456
28°	58.58	59.63	1.0179
30°	53.51	58.44	1.1015
32°	47.84	56.95	1.1906
34°	43.51	34.55	0.7941
36°	39.30	29.82	0.7588
38°	34.55	-----	------
40°	31.66	27.69	0.8746

*All data recorded at a measured flow rate of approximately 1.78 lb_m/sec. Ribbed wall configuration:

A = 0.7 in.

B = 0.125 in.

TH = 0.06

N = 10

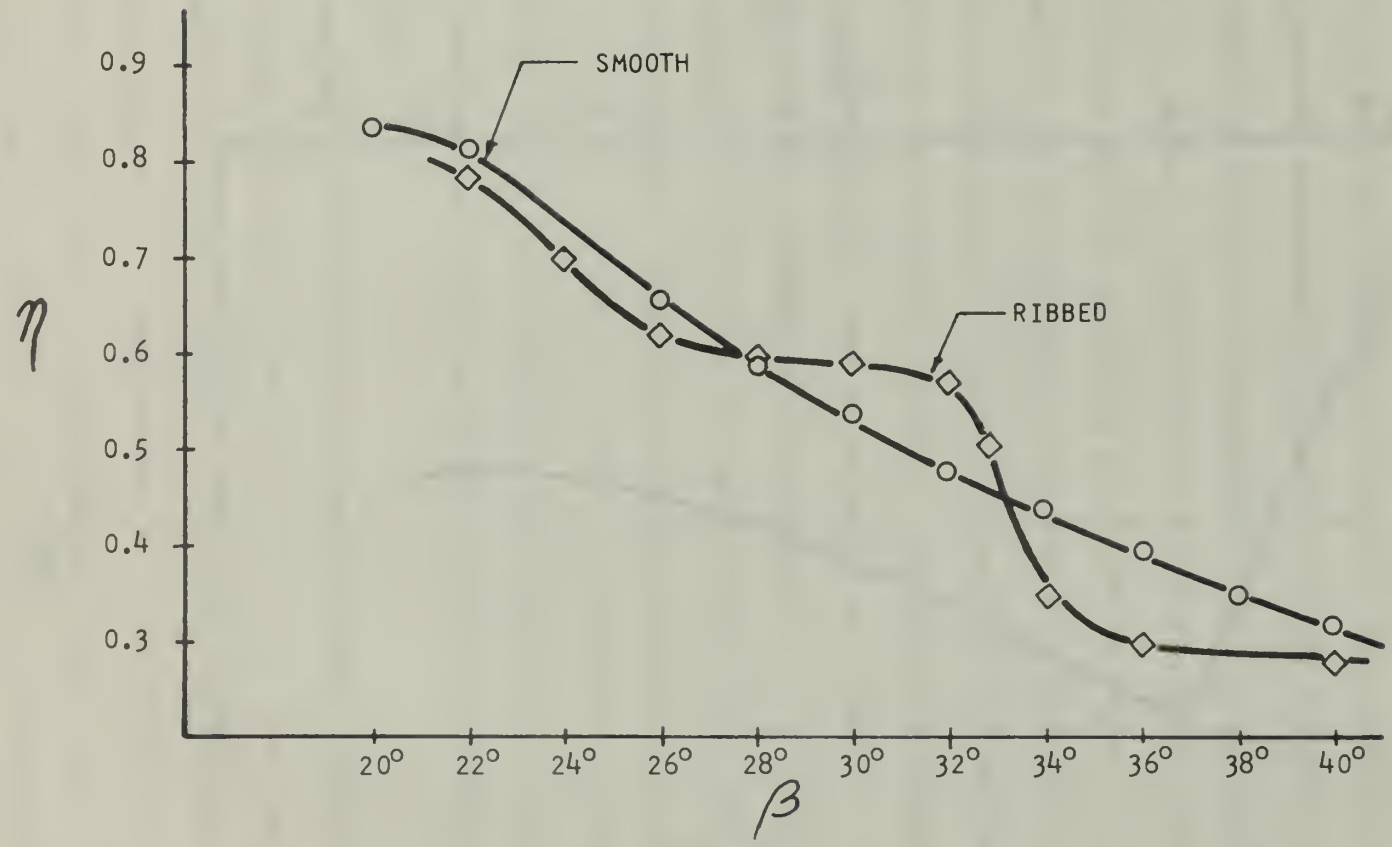


FIGURE 11

SUMMARY OF RIBBED WALL AND SMOOTH WALL DIFFUSOR EFFICIENCIES

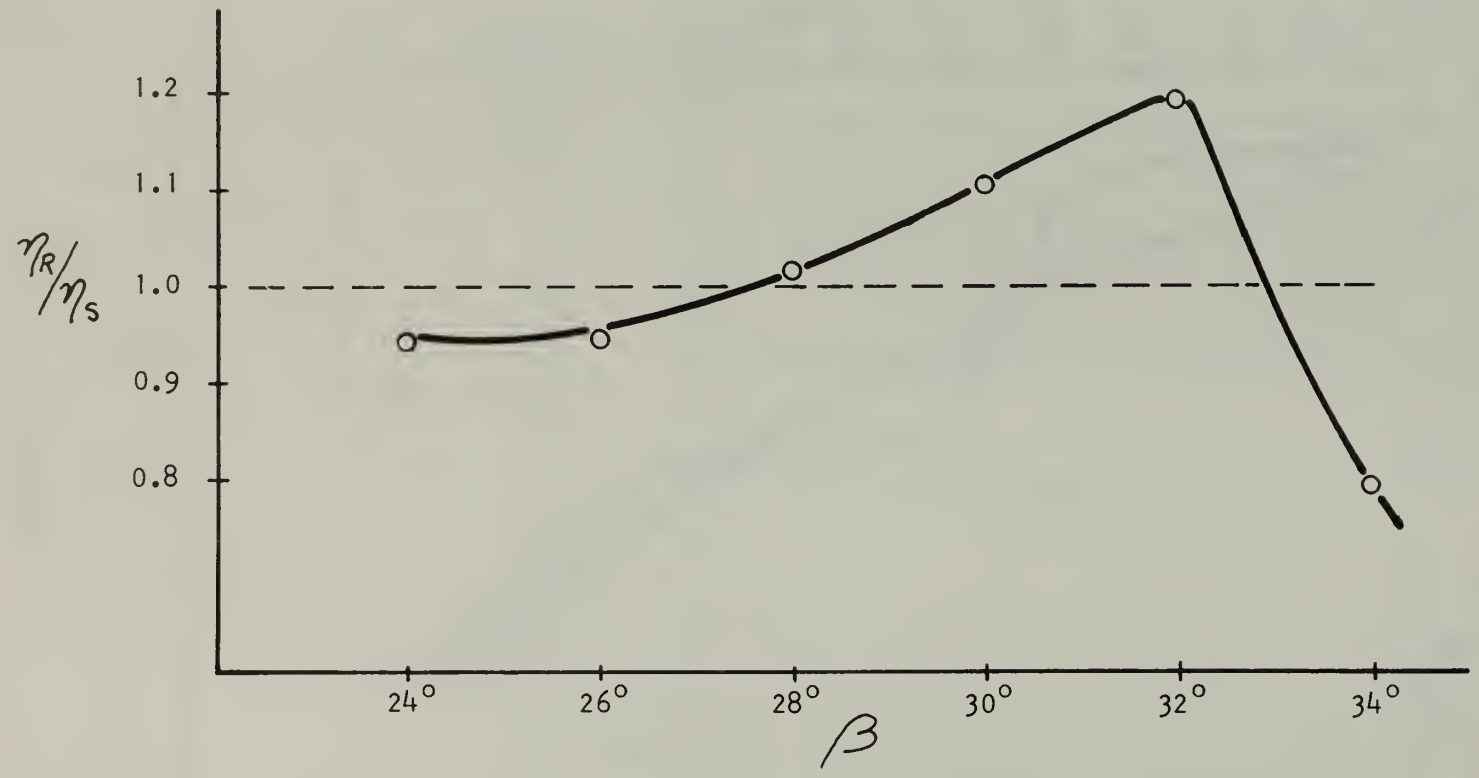


FIGURE 12

RATIO η_R/η_s AS A FUNCTION OF β TO COMPARE THE RIBBED WALL DIFFUSOR PERFORMANCE TO THAT OF A SMOOTH WALL DIFFUSOR

4.1.3 Effect of varying the number of grooves upon ribbed wall diffusor performance. Table VI is the result of the third and final phase of this investigation. Unfortunately, time did not permit this phase of the testing to proceed beyond N = 10 grooves. One interesting result of these tests is illustrated in Table VI. At $\beta = 30^{\circ}$ and $\beta = 32^{\circ}$, it was noted that the efficiency of the ribbed wall diffusor decreased by approximately 20 per cent as the number of grooves was increased from 7 to 8. This phenomenon did not occur at $\beta = 30^{\circ}$. Migay, Ref. 1, reports a similar drop in efficiency for a three dimensional conical diffusor operating at an opening angle of 31 degrees. His explanation for this decrease in efficiency is that it is caused by "acoustic irradiation of inner-fin hollows." No attempt was made in this study to either explain or further investigate the phenomenon.

4.2 Recommendations. Much experimental work remains to be done in the investigation of ribbed walled diffusors. It is hoped that continued studies in this field will make available data upon which a theoretical analysis of ribbed wall diffusor performance can be based.

It is felt that the next step in the investigation of ribbed wall diffusors should be an attempt to obtain data reflecting the effect on performance as other parameters of the rib configuration are varied.

In conjunction with further experimental studies into the effect of ribs on the performance of diffusors, it is felt that studies into the mechanism of flow past grooves or ribs should be thoroughly investigated. Fox, Ref. 10, has done much work in this field. It is felt that the results of his study would be of great value in attempting to understand the mechanism of the ribbed wall diffusor operation.

TABLE VI

EFFECT OF VARYING THE NUMBER OF GROOVES UPON THE PERFORMANCE OF A RIBBED WALL DIFFUSOR.*

$\beta = 28^{\circ}$, A = 0.7, B = 0.125, TH = 0.06

η_R/η_S	0.7979	0.9339	0.9507	0.9706	1.0179
N	6	7	8	9	10

$\beta = 30^{\circ}$, A = 0.7, B = 0.125, TH = 0.06

η_R/η_S	0.7443	0.9587	0.8866	1.0525	1.1015
N	6	7	8	9	10

$\beta = 32^{\circ}$, A = 0.7, B = 0.125, TH = 0.06

η_R/η_S	0.5847	0.9505	0.7306	1.1378	1.1906
N	6	7	8	9	10

*All runs for this test made with measured flow rate of approximately 1.78 lb_m/sec.

The possible use of ribs, or grooves, as a means of affecting boundary layer control in a variety of external as well as internal flow situations seems to indicate that further research into the behavior of ribs is warranted. It is hoped that the equipment, procedures, and experience assembled in the course of this study will serve some useful purpose in any such subsequent investigations.

REFERENCES

1. Cocanower, A. B., S. J. Kline, and J. P. Johnston. "A Unified Method for Predicting the Performance of Subsonic Diffusers of Several Geometries." General Motors Research Laboratories Contract AF 49(638)-1278 for Mechanics Division, Air Force Office of Scientific Research. Department of Mechanical Engineering, Stanford University, Stanford, 1965.

2. Waitman, B. A., L. R. Reneau, and S. J. Kline. "Effects of Inlet Conditions on Performance of Two-Dimensional Subsonic Diffusors," Journal of Basic Engineering, 83, September, 1961, pp. 349-60.

3. Moore, Carl A. and Stephen J. Kline. "Some Effects of Vanes and of Turbulence in Two-Dimensional Wide-Angle Subsonic Diffusers," NACA TN 4080, June, 1958.

4. Migay, V. K. "Investigating Finned Diffusors." Russian Periodical, Teploenergetila, Nr. 10, Oct. 1962, Foreign Technology Division, WP-AFB, Ohio (FTD-TT-63-86/1+2).

5. Eshbach, Ovid W. Handbook of Engineering Fundamentals, Second Edition. New York: John Wiley and Sons, Inc., 1965.

6. Supplement to ASME Power Test Codes, Chapter 4, Part 5, ASME, New York, 1959.

7. Stearnes, R. F., et al. Flow Measurement with Orifice Meters, New York: van Nostrand Co., Inc., 1951.

8. VDI Durchfluss Messregeln (Flow Nozzle Measurements) DIN 1952, VDI Verlag, Berlin, 1943.

9. Schlichting, Herman. Boundary Layer Theory, Fourth Edition. New York: McGraw Hill Book Co., Inc., 1960.

10. Fox, Jay. "Surface Pressure and Turbulent Airflow in Transverse Rectangular Notches," NASA TN D-2501, November, 1964.

APPENDIX A

COMPUTER PROGRAM

General statements concerning program "Diffusor." All of the calculations discussed in Chapter III were programmed for the IBM 360-67 Digital Computer in operation at the Computer Facility, Naval Postgraduate School, Monterey. The program was written in Fortran IV language. All of the calculations as discussed in Chapter III are utilized in the program named "Diffusor." Appendix B is a listing of the program. Included in the program listing are "comment" cards to help explain each step of the calculation. A basic understanding of the Fortran IV language should be all that is required to follow the program operation. In this Appendix the emphasis is directed toward the input and output phase of the program operation.

Program input. The special listing of symbols entitled "Program Input Variables" included with this Appendix defines the Fortran variables names used as input for program "Diffusor." Figure 13 is a sample data page illustrating the order and variable names as recorded during the tests. Figure 14 shows the field specification for each of the input variables.

The first data card of each program run is a 72 space "Hollerith" statement. The first 72 spaces of this card may be utilized to include supplementary or amplifying statements to be printed as part of the program output. Any information punched on this card will be reproduced directly beneath the title line on the output page.

PROGRAM INPUT VARIABLES

MM	Number of sets of data to be read
IRUN	Number of run
MO	Month (numeric)
IDAY	Day of month (numeric)
PATM	Atmospheric pressure
PINOZ	Static pressure ahead of nozzle (P_u)
DLTP	Pressure drop across nozzle (ΔP)
TN	Total temperature at nozzle
TEMP	Temperature (^{o}C) for PATM correction
PI	Static pressure at inlet P_1
QI	Dynamic head at inlet (P_t-P_1)
TTI	Total temperature at inlet (T_{t1})
BETA	Total diffusor opening angle
TPR	Outside ambient air temperature (^{o}F)
AA	Depth of grooves
BB	Width of grooves
TH	Spacing between grooves
NN	Number of grooves

UNITED STATES
NAVAL POSTGRADUATE SCHOOL

TURBO-PROPULSION LABORATORY
DEPARTMENT OF AERONAUTICS

PAGE one OF one

TEST DESCRIPTION: Diffusor (with ribs)*

DATE: 2-13-68

RUN NO: 207

Run/Mo/Day	PATM (In. Hg.)	PINØZ	DLTP	TN (mv)	TEMP (°C)		P1	Q1	TT1 (mv)	β	TPR (°F)		
207/2/13	29.83	12.35	18.95	1.50	22.0		-0.85	2.155	1.50	32.0	57.5		

* B = .125"
A = 0.7"
T = 0.06"
N = 10

FIGURE 13

SAMPLE DATA SHEET

TURBO-MACHINE DATA PGS 145 (4-66)

1	72
SAMPLE INPUT/OUTPUT DATA FOR PROGRAM DIFFUSOR	
72 Space Hollerith Statement Card	

1 2	
1	
MM	

1 3	4 6	7 9	10 19	20 29	30 39	40 49	50 59
207	02	13	29.83	12.35	18.95	1.50	22.0
IRUM	MO	IDAY	PATM	PINOZ	DLTP	TN	TEMP

1 10	11 20	21 30	31 40	41 50
-0.850	2.155	1.50	32.0	57.5
P1	Q1	TT1	BETA	TPR

1 10	11 20	21 30	31 40
0.70	0.125	0.06	10
AA	BB	TH	NN

FIGURE 14

INPUT DATA FIELD AND FORMAT SPECIFICATIONS FOR PROGRAM DIFFUSOR
(Top line indicates card spacing)

The second data card of each computer run will indicate the number of data sets which are to be read. The name given to this "fixed point" variable is MM.

The remaining data cards represent the input to the program. Each data point requires three cards. As illustrated in Fig. 14, the first of each series of three input cards contains the following: IRUN, MO, IDAY, PATM, PINOZ, DLTP, TN, and TEMP. The second of each series of three cards includes: PI, QI, TTI, BETA, and TPR. The last in the set of three cards used for each data point contains the following information related to the ribs of the diffusor: AA, BB, TH, and NN. The symbols used to identify the input variables are defined in this Appendix. For smooth wall runs, this card was left blank resulting in zeros for all of the rib parameters.

Special attention is directed to the fact that the "I" format variables are right justified within their specified fields whereas the "F format variables can be punched anywhere within the specified field provided the decimal is punched with the number. The field specifications and the format for each of the input variables is included in Fig. 14.

Program output. Figure 15 is a sample of the output from program "Diffusor." The same data used to illustrate the input in Figs. 13 and 14 are printed as output in Fig. 15.

The second line of output is the Hollerith statement read into the program as the first data card.

The grouping labeled DATA CHECK is a print out of the raw data as read into the program. It was used to check the output for possible errors in card punching.

TWO DIMENSIONAL RIBBED WALL DIFFUSOR PERFORMANCE EVALUATION DATA

SAMPLE INPUT/OUTPUT DATA FOR PROGRAM DIFFUSOR

RUN 207 DATE 2-13-68

CONFIGURATION:

BETA (DIFFUSOR ANGLE)	= 32.0000	DEG
WIDTH OF GROOVES (B)	= 0.1250	IN.
DEPTH OF GROOVES (A)	= 0.7000	IN.
SPACING BETWEEN GROOVES (T)	= 0.0600	IN.
NUMBER OF GROOVES (N)	= 10	

DATA CHECK

PATM=29.830 P1NOZ=12.350 DLTP= 18.950 TN= 1.50 TEMP=22.00 DEG C
P1=-0.850 Q1= 2.155 TT1= 1.50 TPR=57.50

FLOW RATE, MEASURED WITH 3.022 INCH FLOW NOZZLE

INPUT:

P1(NOZZLE)	= 14.9570	PSIA
DELTA PRESSURE	= 0.5477	PSIA
TOTAL TEMPERATURE	= 84.9912	DEG F

OUTPUT:

FLOW RATE (MASS)	= 1.0440	LB/SEC
EQUIVALENT FLOW RATE	= 2.0979	SQ.IN.
REFERED FLOW RATE	= 1.0513	LB/SEC

DIFFUSOR PERFORMANCE DATA

INPUT:

ATMOSPHERIC PRES.	= 14.6000	PSI
P1 (INLET STATIC)	= 14.5755	PSIA
PT1 (INLET TOTAL)	= 14.6377	PSIA
P2 (EXIT STATIC)	= 14.6000	PSIA

OUTPUT:

COEF. OF PRESSURE RECOVERY	= 0.3944	
INLET CONDITIONS:		
VMAX (CENTRAL CORE)	= 89.2520	FT/SEC
DENSITY(CENTRAL CORE)	=.2248E-02	SLUGS/CU FT
REYNOLDS NO. (EQV.DIA.)	=.2088E 06	
MACH NO. (INLET CORE)	= 0.0781	
AREA RATIO (EXIT/INLET)	= 2.5362	
CALCULATED MASS FLOW RATE	= 1.0437	LB/SEC
IDEAL PRES. RECOVERY COEF.	= 0.8445	
EFFICIENCY (USING IDEAL V2)	= 0.4679	
EFFICIENCY (PR/PR IDEAL)	= 0.4670	

DATA RELIABILITY INDICATOR

1.0 - (FLOW RATE MEASURED/FLOW RATE CALCULATED) =-0.0063

FIGURE 15

SAMPLE OUTPUT PROGRAM DIFFUSOR

The input sections under the headings of "Flow Rate" and "Diffusor Performance" are the converted values of the input data.

The output sections under these two headings are those values calculated in accordance with the discussion in Chapter III.

```
FORTRAN IV G LEVEL 1, MOD 0          MAIN                DATE = 68061          05/12/30

C
C    ASSIGN VALUES TO FIXED CONSTANTS NEEDED FOR COMPUTATIONS
C
0001          TSTD=518.7
0002          PSTD=29.92*.4921
0003          TEXAS =.8
0004          G= 32.17
0005          R= 53.35
0006          GAM= 1.4
0007          MM=0
0008          A=2.*G*778.3
C
C    READ IN INPUT DATA AND PRINT OUT FOR DATA CHECK
C
0009          READ (5,1000)
0010          READ (5,10) NUM
0011       15 READ (5,20) IRUN,MO,IDAY,PATM,P1NOZ,DLTP,TN,TEMP
0012          READ (5,25) P1,Q1,TT1,BETA,TPR
0013          READ (5,26) AA,BB,TH,NN
0014          MM=MM+1
0015          WRITE (6,399)
0016          WRITE (6,400)
0017          WRITE (6,1000)
0018          WRITE (6,401) IRUN,MO,IDAY
0019          WRITE (6,402)
0020          WRITE (6,403) BETA
0021          WRITE (6,404) BB
0022          WRITE (6,405)AA
0023          WRITE (6,406) TH
0024          WRITE (6,407) NN
0025          WRITE (6,380)
0026          WRITE (6,381) PATM,P1NOZ,DLTP,TN,TEMP
0027          WRITE (6,382) P1,Q1,TT1,TPR
C
C    CONVERT DATA INTO DIMENSIONALLY CORRECT UNITS OF MEASURE
C
0028          PATM=PATM*(1.-((.0001634*TEMP)/(1.+.0001818*TEMP)))*.4912
0029          P2=PATM
0030          DLTP=DLTP*TEXAS*.03613
0031          P1NOZ=PATM+P1NOZ*TEXAS*.03613
0032          Q1=Q1*TEXAS*.03613
0033          P1=PATM+P1*.03613*TEXAS
0034          PT1=P1+Q1
0035          TT1= 32.+35.98*TT1-.435*TT1**2+459.7
0036          TN= 32.+35.98*TN-.435*TN**2
0037          TNR=TN+459.7
C
C    BEGIN FLOW RATE CALCULATIONS USING FLOW NOZZLE READINGS
C
0038          X=DLTP/P1NOZ
0039          Y=(1.-X)**1.428
0040          Z=(1.-X)**0.286
0041          EPS=SQRT(2.433*Y/X*(1.-Z)/(1.-.305*Y))
0042          FT=1.+.000015*(TN-60.)
0043          WEQIV=11.3*EPS*FT*SQRT(X)
0044          W=WEQIV*P1NOZ*SQRT(G/(R*TNR))
C
C    COMPUTE MACH NUMBER
C
0045          AMACH=SQRT(2./(GAM-1.)*((PT1/P1)**((GAM-1.)/GAM)-1.))
C
C    COMPUTE STATIC TEMPERATURE AT INLET
C
0046          T1=TT1/(1.+(GAM-1.)/2.*AMACH**2)
C
C    COMPUTE VELOCITY IN THE CENTRAL FLOW REGION
C
0047          VMAX=AMACH*SQRT(GAM*R*G*T1)
C
C    COMPUTE THE DENSITY OF THE FLOW IN THE CENTRAL REGION
C
0048          RO=P1*144./(R*G*T1)
C
```

```
C    BEGIN THE NUMERICAL INTEGRATION TO DETERMINE THE FLOW RATE AT THE
C    INLET PLANE
C
0049            WSUBD=0.0
0050            WSUBE= 0.0
0051            WSUBF= 0.0
0052            H=-.025
0053            DO 100 N=1,116,5
0054            H=H+.05
0055            V=VMAX*(1.-.01667*(ALOG(1.2/H))**2)
0056          100 WSUBF=RO*G*V*.05*4.8/144.+WSUBF
0057            WF=2.*WSUBF
0058            WC=RO*G*VMAX*4.8*1.6/144.
0059            H=-.025
0060            DO 200 N=1,56,5
0061            H=H+.05
0062            V=VMAX*(1.-.03333*(ALOG(.60/H))**2)
0063            WSUBD=RO*G*V*.05*1.6/144.+WSUBD
0064            H1=-.025
0065            DO 200 J=1,116,5
0066            H1=H1+.05
0067            V=VMAX*(1.-.01667*(ALOG(1.2/H1))**2)*(1.-.03333*(ALOG(.6/H))**2)
0068          200 WSUBE=RO*G*V*.0025/144.+ WSUBE
0069            WE=WSUBE*4.
0070            WD=2.*WSUBD
0071            WCALC=WC+WD+WE+WF
C
C    COMPUTE THE COEFFICIENT OF PRESSURE RECOVERY
C
0072            CPR=(P2-P1)/Q1
C
C    COMPUTE THE AREA RATIO OF THE DIFFUSOR FOR THE SPECIFIED OPENING
C    ANGLE
C
0073            BETA=BETA/57.3
0074            ALFA=BETA/2.
0075            BETA=BETA*57.3
0076            ARATIO=.33333*(3.1875+16.1*TAN(ALFA)-.1875/COS(ALFA))
C
C    COMPUTE REYNOLDS NUMBER BASED UPON MIDSTREAM VELOCITY AND THE
C    HYDRAULIC DIAMETER OF THE INLET FLOW CHANNEL
C
0077            VIS=.0000016*(TT1-459.7)+.00012
0078            RE=VMAX*.4/VIS
C
C    COMPUTE THE IDEAL COEFFICIENT OF PRESSURE RECOVERY
C
0079            PRSTAR=1.-(1./ARATIO)**2
C
C    COMPUTE THE REFERRED FLOW RATE (NORMALIZED TO STANDARD DAY
C    CONDITIONS)
C
0080            TPR=TPR+459.7
0081            WSTD=W*SQRT(TPR/TSTD)/(PATM/PSTD)
C
C    COMPUTE THE VELOCITY AT THE EXIT BASED UPON AN IDEAL EXPANSION
C    OF THE MID STREAM FLOW
C
0082            V2=VMAX/ARATIO
C
C    COMPUTE EFFICIENCY BASED UPON THE DEFINITION OF EQ(3-28)
C
0083            EFNCY=(P2-P1)*144./(.5*RO*(VMAX**2-V2**2))
C
C    COMPUTE EFFICIENCY BASED UPON THE IDEAL COEFFICIENT OF PRESSURE
C    RECOVERY
C
0084            EFFN2= CPR/PRSTAR
C
C    DETERMINE THE DATA RELIABILITY INDICATOR
C
0085            ERR= 1.0 -(W/WCALC)
C
```

```
FORTRAN IV G LEVEL 1, MOD 0             MAIN                DATE = 68061          05/12/30

C    PRINT ALL VALUES AS COMPUTED
C
0086          WRITE (6,408)
0087          WRITE (6,409)
0088          WRITE (6,410) PINOZ,W
0089          WRITE (6,411) DLTP,WEQIV
0090          WRITE (6,412) TN,WSTD
0091          WRITE (6,413)
0092          WRITE (6,409)
0093          WRITE (6,414) PATM,CPR
0094          WRITE (6,415) P1
0095          WRITE (6,416) PT1,VMAX
0096          WRITE (6,417) P2,RO
0097          WRITE (6,418) RE
0098          WRITE (6,419) AMACH
0099          WRITE (6,420) ARATIO
0100          WRITE (6,421) WCALC
0101          WRITE (6,423) PRSTAR
0102          WRITE (6,424) EFNCY
0103          WRITE (6,425) EFFN2
0104          WRITE (6,426)
0105          WRITE (6,427) ERR
0106          IF (MM.LT.NUM) GO TO 15
0107       10 FORMAT (I2)
0108       20 FORMAT (3I3,5F10.4)
0109       25 FORMAT (5F10.4)
0110       26 FORMAT (3F10.4,I10)
0111      380 FORMAT (15X,'DATA CHECK'/)
0112      381 FORMAT (25X,'PATM=',F6.3,'     PINOZ=',F6.3,'     DLTP=',F7.3,'
             1  TN=',F5.2,'     TEMP=',F5.2,'  DEG C')
0113      382 FORMAT (25X,'P1=',F6.3,'    Q1=',F6.3,'    TT1=',F5.2,'    TPR=',F
             15.2//)
0114      399 FORMAT (1H1/////)
0115      400 FORMAT (30X,  'TWO DIMENSIONAL RIBBED WALL DIFFUSOR PERFORMANCE EV
             1ALUATION DATA'//)
0116      401 FORMAT (15X,4HRUN ,I3,80X,5HDATE ,I2,1H-,I2,3H-68/////)
0117      402 FORMAT (15X,'CONFIGURATION:'/)
0118      403 FORMAT (25X,'BETA (DIFFUSOR ANGLE)        =',F10.4,'  DEG')
0119      404 FORMAT (25X,'WIDTH OF GROOVES (B)         =',F10.4,'  IN.')
0120      405 FORMAT (25X,'DEPTH OF GROOVES (A)         =',F10.4,'  IN.')
0121      406 FORMAT (25X,'SPACING BETWEEN GROOVES (T) =',F10.4,'  IN.')
0122      407 FORMAT (25X,'NUMBER OF GROOVES (N)        =  ',I3//)
0123      408 FORMAT (15X,'FLOW RATE, MEASURED WITH 3.022 INCH FLOW NOZZLE'/)
0124      409 FORMAT (20X,'INPUT:',39X,'OUTPUT:')
0125      410 FORMAT (25X,'P1(NOZZLE)           =',F8.4,'  PSIA',13X,'FLOW RATE (MA
             1SS)     =',F7.4,'  LB/SEC')
0126      411 FORMAT (25X,'DELTA PRESSURE     =',F8.4,'  PSIA',13X,'EQUIVALENT FL
             1OW RATE=',F7.4,'  SQ.IN.')
0127      412 FORMAT (25X,'TOTAL TEMPERATURE =',F8.4,'  DEG F',12X,'REFERED FLOW
             1 RATE   =',F7.4,'  LB/SEC'//)
0128      413 FORMAT (15X,'DIFFUSOR PERFORMANCE DATA'/)
0129      414 FORMAT(25X,'ATMOSPHERIC PRES.  =',F8.4,'  PSI ',11X,' COEF. OF PRE
             1SSURE RECOVERY  =',F9.4)
0130      415 FORMAT (25X,'P1 (INLET STATIC) =',F8.4,'  PSIA',12X,' INLET CONDIT
             1IONS:')
0131      416 FORMAT (25X,'PT1 (INLET TOTAL) =',F8.4,'  PSIA',12X,'       VMAX (C
             1ENTRAL CORE)     =',F9.4,'  FT/SEC')
0132      417 FORMAT (25X,'P2 (EXIT STATIC)  =',F8.4,'  PSIA',12X,'       DENSITY
             1(CENTRAL CORE)  =',E9.4,'  SLUGS/CU FT')
0133      418 FORMAT (76X,'REYNOLDS NO. (EQV.DIA.)=',E9.4)
0134      419 FORMAT (76X,'MACH NO. (INLET CORE)  =',F9.4)
0135      420 FORMAT (71X,'AREA RATIO (EXIT/INLET)      =',F9.4)
0136      421 FORMAT (71X,'CALCULATED MASS FLOW RATE    =',F9.4,'  LB/SEC')
0137      423 FORMAT (71X,'IDEAL PRES. RECOVERY COEF.   =',F9.4)
0138      424 FORMAT (71X,'EFFICIENCY (USING IDEAL V2) =',F9.4)
0139      425 FORMAT (71X,'EFFICIENCY (PR/PR IDEAL)     =',F9.4)
0140      426 FORMAT (//15X,'DATA RELIABILITY INDICATOR'/)
0141      427 FORMAT (25X,'1.0 - (FLOW RATE MEASURED/FLOW RATE CALCULATED) =',F7
             1.4)
0142     1000 FORMAT (72H
             1                    )
0143          END
```

INITIAL DISTRIBUTION LIST

		No. Copies
1.	Defense Documentation Center Cameron Station Alexandria, Virginia 22314	20
2.	Library Naval Postgraduate School Monterey, California	2
3.	Commander, Naval Air Systems Command Navy Department Washington, D.C. 20360	1
4.	Professor R. D. Zucker Department of Aeronautics Naval Postgraduate School Monterey, California	1
5.	Chairman, Department of Aeronautics Naval Postgraduate School Monterey, California	1
6.	Professor A. E. Fuhs Department of Aeronautics Naval Postgraduate School Monterey, California	1
7.	LT Gary L. Beck 242 Via Gayuba Monterey, California 93940	1
8.	Professor M. H. Vavra Department of Aeronautics Naval Postgraduate School Monterey, California	1

DOCUMENT CONTROL DATA - R&D

(Security classification of title, body of abstract and indexing annotation must be entered when the overall report is classified)

1. ORIGINATING ACTIVITY (Corporate author)
Naval Postgraduate School
Monterey, California 93940

2a. REPORT SECURITY CLASSIFICATION
Unclassified

2b. GROUP

3. REPORT TITLE
AN EXPERIMENTAL DETERMINATION OF TWO DIMENSIONAL RIBBED WALL DIFFUSOR PERFORMANCE

4. DESCRIPTIVE NOTES (Type of report and inclusive dates)
Thesis

5. AUTHOR(S) (Last name, first name, initial)
Gary L. BECK, LT, USN

6. REPORT DATE	7a. TOTAL NO. OF PAGES	7b. NO. OF REFS
March 1968	58	10

8a. CONTRACT OR GRANT NO.	9a. ORIGINATOR'S REPORT NUMBER(S)
b. PROJECT NO.	
c.	9b. OTHER REPORT NO(S) (Any other numbers that may be assigned this report)
d.	

10. AVAILABILITY/LIMITATION NOTICES
[redacted]

11. SUPPLEMENTARY NOTES	12. SPONSORING MILITARY ACTIVITY
	Naval Postgraduate School Monterey, California 93940

13. ABSTRACT

The results of tests made with a two dimensional diffusor operating with transverse grooves cut into the diverging side walls were compared with the results of similar tests made using a smooth wall diffusor. The results of this comparison revealed that:

1. The efficiency of the ribbed wall configuration exceeded that of the smooth wall diffusor for total opening angles of approximately 28 to 33 degrees.
2. The ribbed wall configuration had an efficiency approximately 120 per cent of that of the smooth wall diffusor when both were operated at a total opening angle of 32 degrees.
3. The efficiencies of the ribbed wall diffusor operating at large opening angles varied as a function of the number of grooves in the side walls.
4. The efficiency increased as the number of grooves increased, but an unexplained drop in efficienty occurred at opening angles of 30 and 32 degrees with an eight groove configuration.
5. The maximum number of grooves tested was ten. There is no evidence to indicate that this is an optimum configuration.

DD FORM 1 JAN 64 1473

14 KEY WORDS	LINK A		LINK B		LINK C	
	ROLE	WT	ROLE	WT	ROLE	WT
Ribbed wall diffusor						
Wide angle diffusor						

NO FORN

thesB3275
DUDLEY KNOX LIBRARY
3 2768 00407300 7
DUDLEY KNOX LIBRARY